Hindawi
Journal of Function Spaces
Volume 2021, Article ID 9984473, 11 pages
https://doi.org/10.1155/2021/9984473

Research Article

Nonuniform Finite Difference Scheme for the Three-Dimensional Time-Fractional Black–Scholes Equation

Sangkwon Kim,[1] Chaeyoung Lee,[1] Wonjin Lee,[2] Soobin Kwak,[1] Darae Jeong,[3] and Junseok Kim[1]

[1]*Department of Mathematics, Korea University, Seoul 02841, Republic of Korea*
[2]*Department of Financial Engineering, Korea University, Seoul 02841, Republic of Korea*
[3]*Department of Mathematics, Kangwon National University, Gangwon-do 24341, Republic of Korea*

Correspondence should be addressed to Junseok Kim; cfdkim@korea.ac.kr

Received 24 September 2021; Accepted 29 November 2021; Published 24 December 2021

Academic Editor: Youssri Hassan Youssri

In this study, we present an accurate and efficient nonuniform finite difference method for the three-dimensional (3D) time-fractional Black–Scholes (BS) equation. The operator splitting scheme is used to efficiently solve the 3D time-fractional BS equation. We use a nonuniform grid for pricing 3D options. We compute the three-asset cash-or-nothing European call option and investigate the effects of the fractional-order α in the time-fractional BS model. Numerical experiments demonstrate the efficiency and fastness of the proposed scheme.

1. Introduction

We consider the following 3D version of the time-fractional Black–Scholes (BS) model [1]:

$$\begin{aligned}&\frac{\partial^\alpha u}{\partial t^\alpha}(x,y,z,t)+\mathcal{L}_{\mathrm{BS}}u(x,y,z,t)\\&\quad=0\quad\text{for }(x,y,z,t)\in\Omega\times[0,T),\end{aligned}\tag{1}$$

$$u(x,y,z,T)=u_T(x,y,z),\tag{2}$$

where $u(x,y,z,t)$ is the option value at time t and $u_T(x,y,z)$ is the payoff function at time $t=T$,

$$\frac{\partial^\alpha u}{\partial t^\alpha}(x,y,z,t)=\frac{1}{\Gamma(1-\alpha)}\frac{d}{dt}\int_t^T\frac{u(x,y,z,\xi)-u(x,y,z,T)}{(\xi-t)^\alpha}d\xi,\tag{3}$$

where $0<\alpha<1$ and

$$\begin{aligned}\mathcal{L}_{\mathrm{BS}}=&\frac{1}{2}\sigma_x^2x^2\frac{\partial^2u}{\partial x^2}+\frac{1}{2}\sigma_y^2y^2\frac{\partial^2u}{\partial y^2}+\frac{1}{2}\sigma_z^2z^2\frac{\partial^2u}{\partial z^2}\\&+\rho_{xy}\sigma_x\sigma_yxy\frac{\partial^2u}{\partial x\partial y}+\rho_{yz}\sigma_y\sigma_zyz\frac{\partial^2u}{\partial y\partial z}\\&+\rho_{zx}\sigma_z\sigma_xzx\frac{\partial^2u}{\partial z\partial x}+rx\frac{\partial u}{\partial x}+ry\frac{\partial u}{\partial y}+rz\frac{\partial u}{\partial z}-ru.\end{aligned}\tag{4}$$

Here, x, y, and z, and σ_x, σ_y, and σ_z are the prices and volatilities of the underlying assets x, y, and z, respectively. Additionally, ρ_{xy}, ρ_{yz}, and ρ_{zx} are the correlation values between two subscript asset variables, and r is the interest rate. Black and Scholes published in 1973 their paper which described the BS model and option pricing formula [2]. This has become an important fundamental topic for studying financial engineering and financial theory. However, the option pricing formula is based on the assumption that the returns of asset prices follow a Gaussian distribution. This means that the volatility of the underlying asset price is

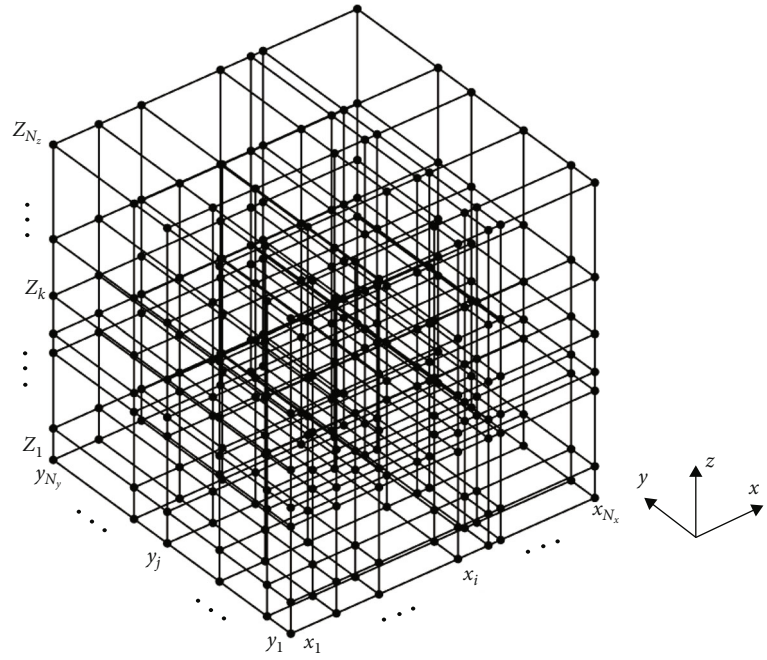

Figure 1: Three-dimensional nonuniform mesh.

constant until the time to maturity of the option contracts. This has become a weakness of this formula. Many researchers and traders have found that rare events such as drastic drops in financial markets are much more frequent than would be anticipated based on Gaussian distributions and that the distribution of the returns of asset prices has a fat tail. Therefore, in real financial markets, many researchers have begun to develop models that more accurately reflect real market. The study of stable distribution has arisen naturally during the study of heavy-tailed distributions and has been applied in finance to develop models of extreme events that occur rarely. Because a stable probability distribution captures unpredictable events well, it is now more suitable for financial markets than the BS model. Time-fractional analysis is closely connected to stable probability distributions [3]. Many researchers in the financial field have attempted to generalize the BS model in the fractional-order based on the fact that fractional derivatives and integrals provide powerful tools for explaining the memory and hereditary traits of different substances. The use of the fractional BS model for the high volatility of the stock market is one such generalization. There are two types of fractional derivatives as space-fractional [4, 5] and time-fractional derivatives [6, 7]. Regarding the time-fractional model, researchers have focused on the analytical [8–10] and numerical [11–13] methods. The finite difference method (FDM) is known as the most famous evaluation tool in quantitative finance and is more stable than Monte Carlo simulation (MCS). FDM has been applied in various studies [14, 15]. One researcher who has solved a two-dimensional time-fractional BS model using an implicit FDM proposed a fast biconjugate gradient stabilized scheme to solve the linear system to speed up computation and save storage space [16]. Option derivatives, European vanilla

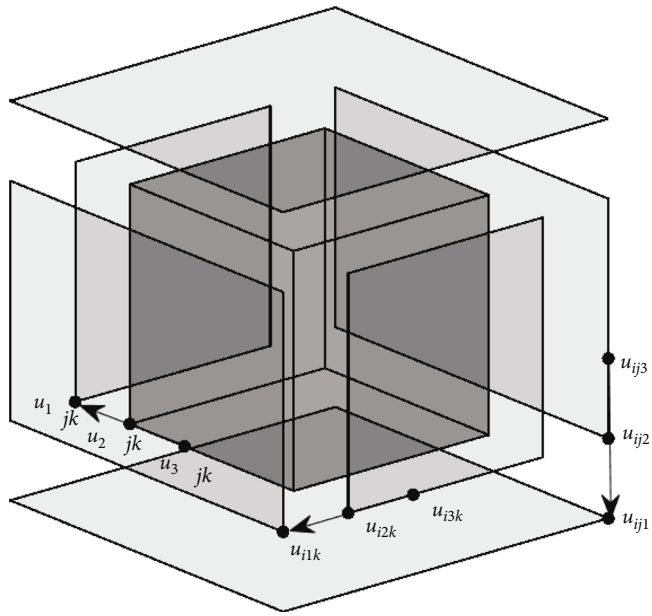

Figure 2: Schematic illustration of the linear boundary condition.

options [17], and double barrier options [18] are analytically priced under the time-fractional BS equation. In [19], the authors developed a homotopy perturbation method to obtain the analytical solutions for the fractional BS equation. Khajehnasiri and Safavi presented the Boubaker operation matrix for the time fractional derivative which approximates the solution of the fractional BS [20]. The authors in [21] proposed a novel operator splitting scheme for pricing American options using the time-fractional BS equation. They provided the effects of the fractional orders and the comparison of fractional equations through the numerical analysis. The paper also used the FDM of the Crank–Nicolson scheme for pricing European

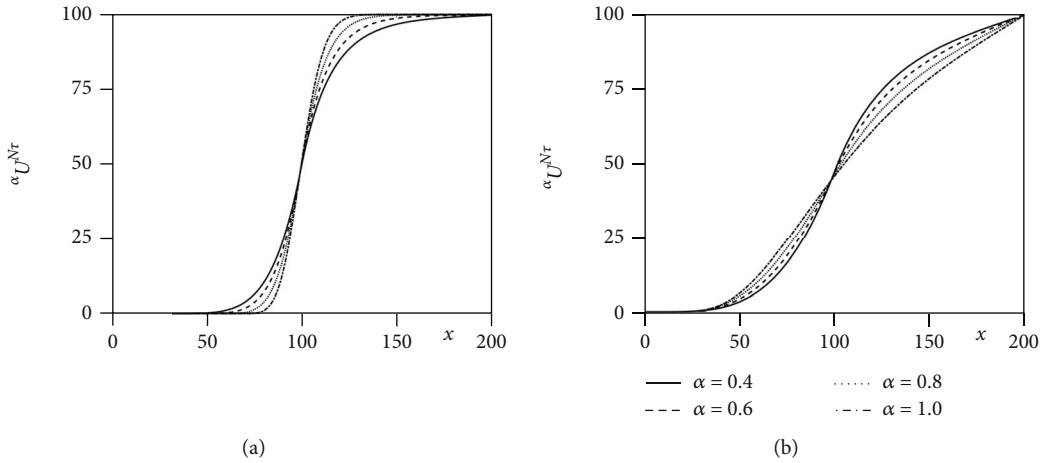

FIGURE 3: Numerical results for cash-or-nothing option for different fractional-orders $\alpha = 0.4,0.6,0.8$, and 1.0 with maturity times (a) $T = 0.1$ and (b) $T = 2.5$.

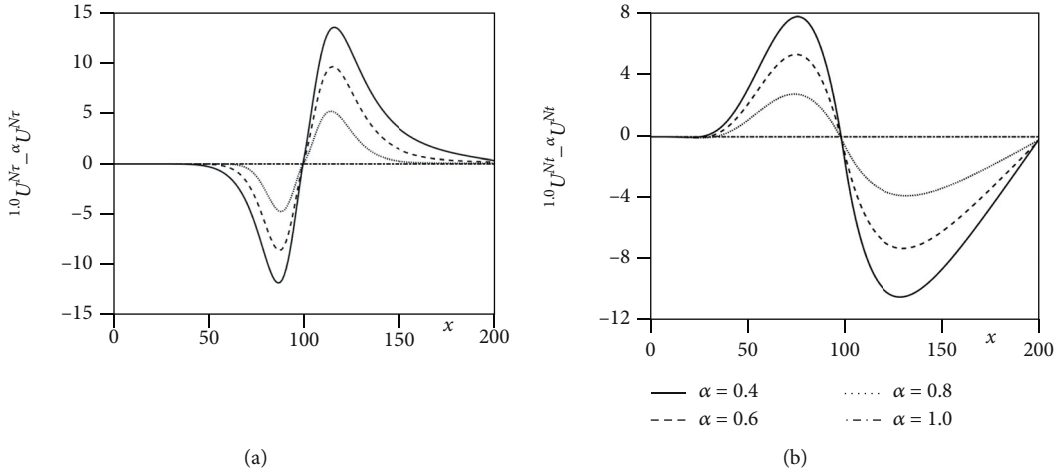

FIGURE 4: Differences in the numerical solutions between $\alpha = 1.0$ and $\alpha = 0.4,0.6,0.8$, and 1.0 for maturity times (a) $T = 0.1$ and (b) $T = 2.5$.

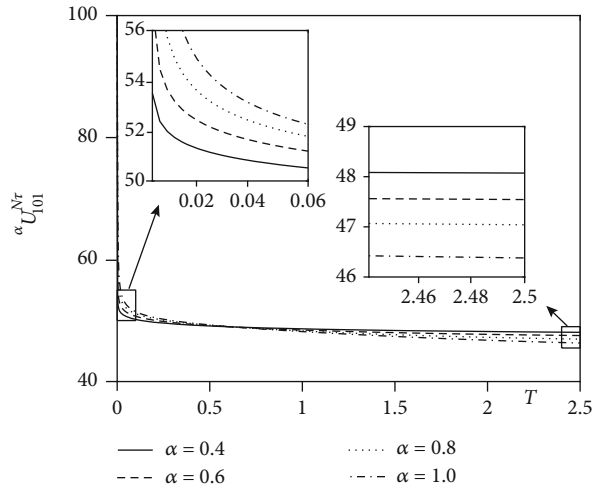

FIGURE 5: Numerical solution at $x = 100$ for maturity $0 \le T \le 2.5$ with $\alpha = 0.4,0.6,0.8$, and 1.0.

options based on the fractional BS equation [22]. They demonstrated that the proposed scheme has unconditional stability and convergent property through the numerical results. In [23], the authors represented that the fractional partial differential equation (PDE) has been successfully applied in option pricing problems and it is more suitable for empirical financial markets. They used a fast preconditioned iterative method for pricing rainbow options based on a two-dimensional fractional PDE. This method demonstrated the accuracy and efficiency of numerical studies. The author in [24] proposed the application of homotopy analysis method (HAM) for pricing European call option based on time-fractional BS equation. He demonstrated the accuracy, effectiveness, and suitability of HAM through comparative tests. The pricing equation based on a space-time fractional PDE is presented in [25]. The author calculated European call and put options based on space-time fractional BS equation using the technique of Adomian decomposition method under the FDM. In [26], option derivatives were numerically priced using the θ-method for the time-fractional BS equation. These schemes are both first-order and second-order accurate in

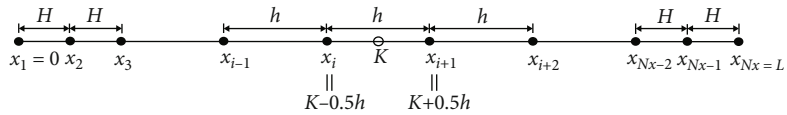

Figure 6: Mesh with a mesh size h for the convergence test.

Table 1: Three-asset cash-or-nothing option prices with varying h and time step $\Delta\tau$.

	$h = 8$	$h = 4$	$h = 2$	$h = 1$
$\Delta\tau = 0.1/10$	21.5301	22.6046	22.9076	22.9860
$\Delta\tau = 0.1/20$	21.4572	22.5433	22.8548	22.9358
$\Delta\tau = 0.1/40$	21.4689	22.5894	22.9176	23.0039
$\Delta\tau = 0.1/80$	21.5070	22.6675	23.0157	23.1082
$\Delta\tau = 0.1/160$	21.5490	22.7479	23.1167	23.2161

time and space, respectively. De Staelen and Hendy [27] improved the spatial fourth-order scheme with a temporal accuracy order of $2 - \alpha$ and performed stability and convergence analysis on their proposed scheme. Golbabai and Nikan [28] numerically solved the time-fractional BS equation using the moving least-squares method. The authors in [29] solved the fractional three-dimensional (3D) chaotic process using the Adams–Bashforth–Moulton (ABM) method. They implemented an alternative numerical method based on the ABM method to reduce the computational cost and demonstrated that the proposed method is efficient and effective. She et al. [30] modified an $L1$ scheme to solve the time-fractional BS equation. The modified $L1$ time method is based on a change of variable and then obtains optimal error estimates. In [31], the authors removed the convection term with exponential transformation, transforming the time-fractional BS model into a time-fractional subdiffusion model, and then applied L 1 -2 formula for the Caputo time-fractional derivative. This scheme applied a quadratic B-spline collocation scheme for space. By using the compact quadratic spline collocation (QSC) scheme, this scheme yields $3 - \alpha$-order and 4-order convergence in time and space, respectively. The complexity of calculations and CPU time are very important when applying numerical methods to solve high-dimensional problems. Although numerical studies have been conducted on the one-asset [26–28] and two-asset [16, 32] options, there is a lack of research on higher-dimensional numerical methods of more than two assets. Therefore, in this paper, we present the 3D time-fractional BS equation for pricing three-asset cash-or-nothing European call option. Let us consider the following change of the variable $\tau = T - t$; then,

$$\begin{aligned}\frac{\partial^\alpha u}{\partial t^\alpha}(x,y,z,t) &= \frac{1}{\Gamma(1-\alpha)}\frac{d}{dt}\int_t^T \frac{u(x,y,z,\xi)-u(x,y,z,T)}{(\xi-t)^\alpha}d\xi \\ &= \frac{-1}{\Gamma(1-\alpha)}\frac{d}{d\tau}\int_{T-\tau}^T \frac{u(x,y,z,\xi)-u(x,y,z,T)}{(\xi-T+\tau)^\alpha}d\xi \\ &= \frac{-1}{\Gamma(1-\alpha)}\frac{d}{d\tau}\int_0^\tau \frac{u(x,y,z,T-\eta)-u(x,y,z,T)}{(\tau-\eta)^\alpha}d\eta,\end{aligned} \tag{5}$$

where $\eta = T - \xi$ is used. Let $U(x,y,z,\tau) = u(x,y,z,T-\tau)$; then, Equation (5) becomes

$$\begin{aligned}&\frac{-1}{\Gamma(1-\alpha)}\frac{d}{d\tau}\int_0^\tau \frac{U(x,y,z,\eta)-U(x,y,z,0)}{(\tau-\eta)^\alpha}d\eta \\ &= \frac{-1}{\Gamma(1-\alpha)}\left[\frac{d}{d\tau}\int_0^\tau \frac{U(x,y,z,\eta)}{(\tau-\eta)^\alpha}d\eta - \frac{d}{d\tau}\int_0^\tau \frac{U(x,y,z,0)}{(\tau-\eta)^\alpha}d\eta\right] \\ &= \frac{-1}{\Gamma(1-\alpha)}\left[\frac{d}{d\tau}\int_0^\tau \frac{U(x,y,z,\eta)}{(\tau-\eta)^\alpha}d\eta - \frac{U(x,y,z,0)}{\tau^\alpha}\right] \\ &= \frac{-1}{\Gamma(1-\alpha)}\frac{d}{d\tau}\int_0^\tau \frac{\partial U(x,y,z,\eta)}{\partial\eta}\frac{(\tau-\eta)^{1-\alpha}}{1-\alpha}d\eta \\ &= \frac{-1}{\Gamma(1-\alpha)}\int_0^\tau \frac{\partial U(x,y,z,\eta)}{\partial\eta}(\tau-\eta)^{-\alpha}d\eta,\end{aligned} \tag{6}$$

where we have used the integration by parts and the Leibniz integral rule. Therefore, after the change of variables, Equation (1) becomes

$$\frac{1}{\Gamma(1-\alpha)}\int_0^\tau (\tau-\eta)^{-\alpha}\frac{\partial U(x,y,z,\eta)}{\partial\eta}d\eta = \mathscr{L}_{\mathrm{BS}}U(x,y,z,\tau), \tag{7}$$

with the initial condition $U(x,y,z,0) = u_T(x,y,z)$ for $(x,y,z,\tau) \in \Omega \times (0,T]$. When we solve the 3D time-fractional BS equation, there are difficulties in terms of memory shortage and computational cost because of the nonlocal property of the temporal derivative, which is the left hand side term in Equation (7). Therefore, we need efficient numerical schemes for this type of time-fractional PDE. First, the numerical scheme should be stable so that relatively large time steps can be used; otherwise, the computational cost will increase exponentially. Second, at each time step, the numerical solution scheme should be fast. To satisfy these conditions, in this study, we present an accurate and efficient nonuniform finite difference method for the 3D time-fractional BS model.

This paper is organized as follows. In Section 2, the proposed numerical scheme is described. In Section 3, numerical results are presented. In Section 4, conclusions are drawn. In the appendix, we provide the MATLAB code for the numerical implementation for the three-asset cash-or-nothing option.

2. Numerical Solutions

Let $\Omega = (0, L_x) \times (0, L_y) \times (0, L_z)$ be the computational domain discretized in nonuniform intervals $h_i^x = x_{i+1} - x_i$, $h_j^y = y_{j+1} - y_j$, and $h_k^z = z_{k+1} - z_k$ for $i = 1, \cdots, N_x - 1$, $j = 1,$

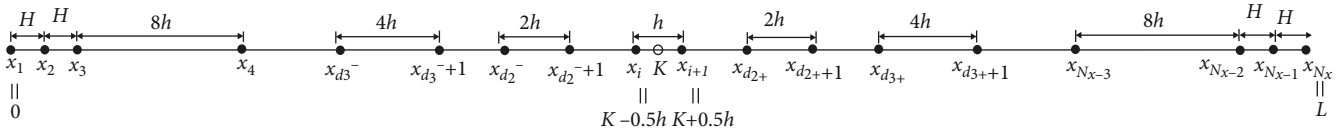

Figure 7: Piecewise-uniform mesh Ω_x.

Table 2: Option prices with respect to α.

α	0.1	0.2	0.3	0.4	0.5
Price	20.6535	21.3818	22.0402	22.6076	23.0786
α	0.6	0.7	0.8	0.9	1.0
Price	23.4597	23.7645	24.0086	24.2053	24.3633

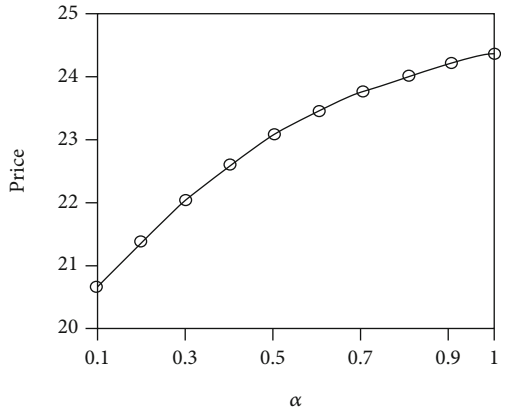

Figure 8: Plot of option prices with respect to α.

$\cdots, N_y - 1$, and $k = 1, \cdots, N_z - 1$. Here, $x_1 = y_1 = z_1 = 0, x_{N_x} = L_x, y_{N_y} = L_y$, and $z_{N_z} = L_z$. $\Delta\tau = T/N_\tau$ is the time step, and N_τ is the number of time steps. Figure 1 illustrates an example of a three-dimensional nonuniform mesh.

Let U_{ijk}^n be the numerical approximation of $U(x_i, y_j, z_k, n\Delta\tau)$ and $\tau_p = p\Delta\tau$. The left hand side term in Equation (7) can be approximated by the following numerical quadrature formula:

$$\begin{aligned}
&\frac{1}{\Gamma(1-\alpha)}\int_0^{\tau_{n+1}} (\tau_{n+1}-\eta)^{-\alpha}\frac{\partial U\left(x_i, y_j, z_k, \eta\right)}{\partial \eta}\, d\eta \\
&= \frac{1}{\Gamma(1-\alpha)}\sum_{p=1}^{n+1}\int_{\tau_{p-1}}^{\tau_p} (\tau_{n+1}-\eta)^{-\alpha}\frac{\partial U\left(x_i, y_j, z_k, \eta\right)}{\partial \eta}\, d\eta \\
&\approx \frac{1}{\Gamma(2-\alpha)}\sum_{p=1}^{n+1}\left[\left(\tau_{n+1}-\tau_{p-1}\right)^{1-\alpha} - \left(\tau_{n+1}-\tau_p\right)^{1-\alpha}\right] \\
&\cdot \frac{U_{ijk}^p - U_{ijk}^{p-1}}{\Delta\tau} = \frac{1}{(\Delta\tau)^\alpha\Gamma(2-\alpha)}\sum_{p=1}^{n+1}\left[(n+2-p)^{1-\alpha}\right. \\
&\left. - (n+1-p)^{1-\alpha}\right]\left(U_{ijk}^p - U_{ijk}^{p-1}\right).
\end{aligned} \tag{8}$$

Therefore, we propose the following discretization of Equation (7) using Equation (8).

$$\begin{aligned}
&\frac{1}{(\Delta\tau)^\alpha\Gamma(2-\alpha)}\sum_{p=1}^{n+1}\left[(n+2-p)^{1-\alpha}\right. \\
&\left. - (n+1-p)^{1-\alpha}\right]\left(U_{ijk}^p - U_{ijk}^{p-1}\right) \\
&= \left(\mathscr{L}_{\mathrm{BS}}^x U\right)_{ijk}^{n+(1/3)} + \left(\mathscr{L}_{\mathrm{BS}}^y U\right)_{ijk}^{n+(2/3)} + \left(\mathscr{L}_{\mathrm{BS}}^z U\right)_{ijk}^{n+1},
\end{aligned} \tag{9}$$

where

$$\begin{aligned}
\left(\mathscr{L}_{\mathrm{BS}}^x U\right)_{ijk}^{n+(1/3)} &= \frac{(\sigma_x x_i)^2}{2} D_{\mathrm{xx}} U_{ijk}^{n+(1/3)} + r x_i D_x U_{ijk}^{n+(1/3)} \\
&+ \sigma_x\sigma_y\rho_{xy} x_i y_j D_{xy} U_{ijk}^n + \sigma_y\sigma_z\rho_{yz} y_j z_k D_{yz} U_{ijk}^n \\
&+ \sigma_z\sigma_x\rho_{zx} z_k x_i D_{zx} U_{ijk}^n - \frac{1}{3} r U_{ijk}^{n+(1/3)}, \\
\left(\mathscr{L}_{\mathrm{BS}}^y U\right)_{ijk}^{n+(2/3)} &= \frac{\left(\sigma_y y_j\right)^2}{2} D_{yy} U_{ijk}^{n+(2/3)} + r y_j D_y U_{ijk}^{n+(2/3)} \\
&- \frac{1}{3} r U_{ijk}^{n+(2/3)}, \\
\left(\mathscr{L}_{\mathrm{BS}}^z U\right)_{ijk}^{n+1} &= \frac{(\sigma_z z_k)^2}{2} D_{zz} U_{ijk}^{n+1} + r z_k D_z U_{ijk}^{n+1} - \frac{1}{3} r U_{ijk}^{n+1}.
\end{aligned} \tag{10}$$

The numerical derivatives are defined as

$$\begin{aligned}
D_x U_{ijk} &= -\frac{h_i^x U_{i-1,jk}}{h_{i-1}^x(h_{i-1}^x + h_i^x)} + \frac{(h_i^x - h_{i-1}^x)U_{ijk}}{h_{i-1}^x h_i^x} + \frac{h_{i-1}^x U_{i+1,jk}}{h_i^x(h_{i-1}^x + h_i^x)}, \\
D_{xx} U_{ijk} &= \frac{2U_{i-1,jk}}{h_{i-1}^x(h_{i-1}^x + h_i^x)} - \frac{2U_{ijk}}{h_{i-1}^x h_i^x} + \frac{2U_{i+1,jk}}{h_i^x(h_{i-1}^x + h_i^x)}, \\
D_{xy} U_{ijk} &= \frac{U_{i+1,j+1,k} - U_{i-1,j+1,k} - U_{i+1,j-1,k} + U_{i-1,j-1,k}}{h_i^x h_j^y + h_{i-1}^x h_j^y + h_i^x h_{j-1}^y + h_{i-1}^x h_{j-1}^y},
\end{aligned} \tag{11}$$

and the other terms are similarly defined. Additional details can be found in [33, 34]. We solve the discrete Equation (9) using the operator splitting method. First, let

$$\begin{aligned}
&\frac{1}{(\Delta\tau)^\alpha\Gamma(2-\alpha)}\sum_{p=1}^{n+1}\left[(n+2-p)^{1-\alpha} - (n+1-p)^{1-\alpha}\right] \\
&\cdot \left(U_{ijk}^p - U_{ijk}^{p-1}\right) = F_{ijk}^n + \frac{U_{ijk}^{n+1} - U_{ijk}^n}{(\Delta\tau)^\alpha\Gamma(2-\alpha)},
\end{aligned} \tag{12}$$

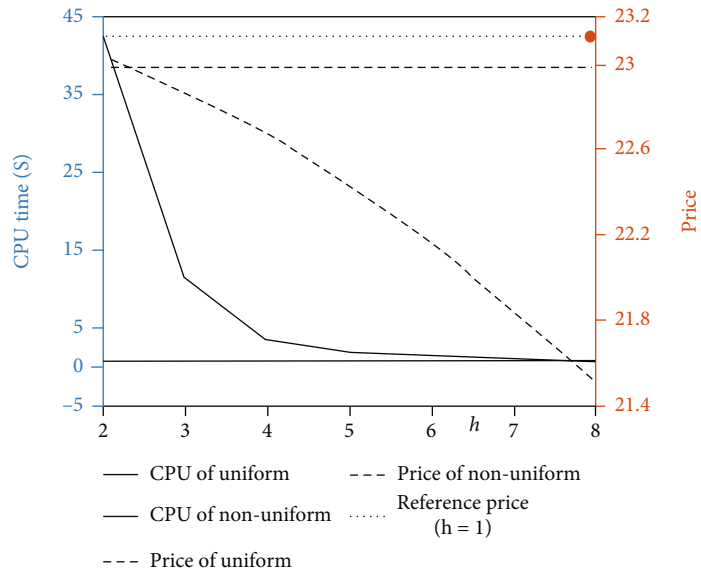

Figure 9: CPU time and price of three-asset cash-or-nothing option for nonuniform mesh with $m_1 = 1, m_2 = 2$, and $m_3 = 3, m_4 = 1$ and uniform mesh with respect to $h = 2, 3, \cdots, 8$.

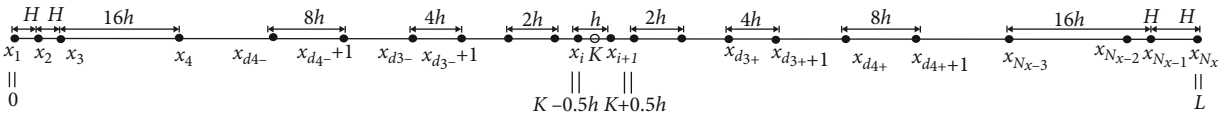

Figure 10: Nonuniform mesh in a comparison test.

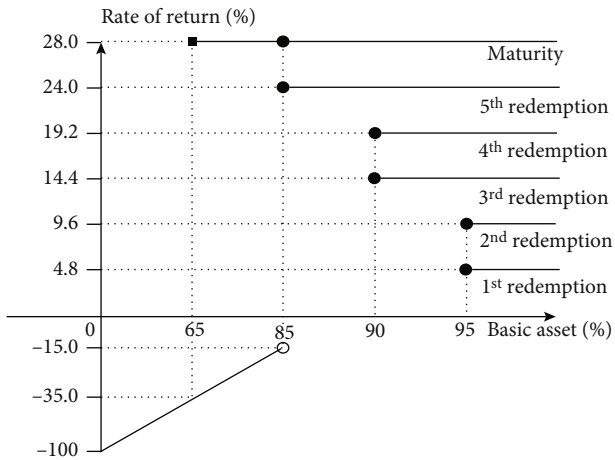

Figure 11: ELS payoff structure.

where

$$F_{ijk}^{n} = \frac{1}{(\Delta\tau)^{\alpha}\Gamma(2-\alpha)} \sum_{p=1}^{n} \left[(n+2-p)^{1-\alpha} - (n+1-p)^{1-\alpha}\right] \left(U_{ijk}^{p} - U_{ijk}^{p-1}\right). \tag{13}$$

Let $\delta\tau = (\Delta\tau)^{\alpha}\Gamma(2-\alpha)$ for simplicity of exposition; then we sequentially solve the following equations [34]:

$$\frac{U_{ijk}^{n+(1/3)} - U_{ijk}^{n}}{\delta\tau} = \left(\mathscr{L}_{\mathrm{BS}}^{x} U\right)_{ijk}^{n+(1/3)} - F_{ijk}^{n}, \tag{14}$$

$$\frac{U_{ijk}^{n+(2/3)} - U_{ijk}^{n+(1/3)}}{\delta\tau} = \left(\mathscr{L}_{\mathrm{BS}}^{y} U\right)_{ijk}^{n+(2/3)}, \tag{15}$$

$$\frac{U_{ijk}^{n+1} - U_{ijk}^{n+(2/3)}}{\delta\tau} = \left(\mathscr{L}_{\mathrm{BS}}^{z} U\right)_{ijk}^{n+1}, \tag{16}$$

for $1 \le i \le N_x$, $1 \le j \le N_y$, and $1 \le k \le N_z$. Note that if we sum up these three equations (14)–(16), then we obtain Equation (9). For the detailed numerical solution, algorithm with source program code of Equations (14)–(16) can be found in [34]. We use the linear boundary condition, specifically, for example, in the case of Equation (14) (see Figure 2):

$$U_{1jk}^{n+(1/3)} = 2U_{2jk}^{n+(1/3)} - U_{3jk}^{n+(1/3)},$$
$$U_{N_x jk}^{n+(1/3)} = 2U_{N_x-1,jk}^{n+(1/3)} - U_{N_x-2,jk}^{n+(1/3)},$$
$$\text{for } j = 2, \cdots, N_y - 1, k = 2, \cdots, N_z - 1,$$

$$U_{i1k}^{n+(1/3)} = 2U_{i2k}^{n+(1/3)} - U_{i3k}^{n+(1/3)},$$
$$U_{iN_y k}^{n+(1/3)} = 2U_{i,N_y-1,k}^{n+(1/3)} - U_{i,N_y-2,k}^{n+(1/3)},$$
$$\text{for } i = 1, \cdots, N_x, k = 2, \cdots, N_z - 1,$$

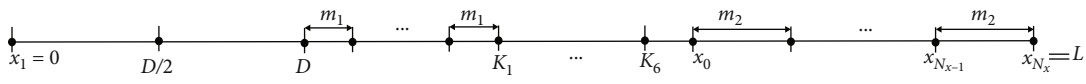

Figure 12: Nonuniform mesh for the three-asset ELS.

$$
\begin{aligned}
U_{ij1}^{n+(1/3)} &= 2U_{ij2}^{n+(1/3)} - U_{ij3}^{n+(1/3)},\\
U_{ijN_z}^{n+(1/3)} &= 2U_{ij,N_z-1}^{n+(1/3)} - U_{ij,N_z-2}^{n+(1/3)},\\
&\text{for } i = 1, \cdots, N_x, j = 1, \cdots, N_y.
\end{aligned}
\tag{17}
$$

3. Numerical Experiments

Numerical experiments were conducted using MATLAB R2020b software on an Intel(R) Core(TM) i7-7700 CPU @3.60 GHz machine with 8 GB of memory.

3.1. Effect of Fractional-Order α. In this subsection, we investigate the effects of the fractional-order α by considering one-asset cash-or-nothing European call option. The payoff function of cash-or-nothing European call option is defined as

$$
U^0(x) = \begin{cases} c, & \text{if } C \geq K,\\ 0, & \text{otherwise,} \end{cases}
\tag{18}
$$

where the strike price is $K = 100$ and the cash is $C = 100$. The parameter values are $r = 0.03$, $\sigma = 0.3$, and $\Delta\tau = 1/365$. We use a uniform mesh $h = 1$ with $L = 200$. Let ${}^{\alpha}U_i^n$ be the numerical approximation of the solution, where $i = 1, \cdots, N_x$, $n = 0, \cdots, N_\tau$, and $0 < \alpha \leq 1$. A linear boundary condition can be applied. Figure 3 illustrates the numerical solutions of cash-or-nothing European call option for different fractional-orders $\alpha = 0.4,0.6,0.8$, and 1.0. Figures 3(a) and 3(b) show the numerical results with a relatively short maturity $T = 0.1$ and long maturity $T = 2.5$, respectively. We can observe the different solution profiles according to α.

Figures 4(a) and 4(b) show the differences in the numerical solutions between $\alpha = 1.0$ and $\alpha = 0.4,0.6,0.8,1.0$, i.e., ${}^{1.0}U^{N\tau} - {}^{\alpha}U^{N\tau}$, for $T = 0.1$ and $T = 2.5$, respectively. The lower the α for a short maturity option, the higher the price of the option is in in the money (ITM) and undervalued in out of the money (OTM), see Figure 4(a). However, for long maturity option, the result is contrary to the result of short maturity option (see Figure 4(b)).

Figure 5 shows numerical solutions at $x = 100$ with $\alpha = 0.4,0.6,0.8$, and 1.0 as maturity increases, $0 \leq T \leq 2.5$. For short maturity times, the solutions with lower α values diffuse rapidly, but as the maturity time increases, the solutions with lower α values diffuse slowly. The results of the two subaxes in Figure 5 can be interpreted similarly to Figure 4.

3.2. Three-Asset Options with Nonuniform Mesh

3.2.1. Cash-or-Nothing Option. We investigated three-asset cash-or-nothing European call option with the following payoff function:

$$
U^0(x, \mathrm{y}, z) = \begin{cases} c, & \text{if } x \geq K_1, y \geq K_2, z \geq K_3,\\ 0, & \text{otherwise,} \end{cases}
\tag{19}
$$

where the strike prices are $K_1 = K_2 = K_3 = 100$ and the cash is $c = 100$. The parameter values are $T = 0.1$, $r = 0.03$, $L = M = N = 200$, $\sigma_x = 0.3$, $\sigma_y = 0.3$, $\sigma_z = 0.3$, and $\rho_{xy} = 0.5$, $\rho_{yz} = 0.5$, and $\rho_{zx} = 0.5$. Figure 6 shows the mesh structure with a mesh size h for the convergence test. Note that we straddle the strike point such that the strike point is in the middle of two neighboring points. If $x_2 < h$, then we reset $x_2 = 0.5x_3$ so that we can apply the linear boundary condition. Similarly, if $x_{N_x} - x_{N_x-1} < h$, then we reset $x_{N_x-1} = 0.5(x_{N_x} + x_{N_x-2})$.

Table 1 presents the three-asset cash-or-nothing European call option prices with various variable h and time step $\Delta\tau$. Here, we use $\alpha = 0.5$. We can confirm that the option prices obtained with each h value converge as the time step $\Delta\tau$ becomes smaller. We adopt the reference solution $U(x_i, y_j, z_k, T)$ which uses $h = 1$ and time step $\Delta\tau = 0.1/80$.

We consider the piecewise-uniform mesh $\Omega_x = \Omega_1 \cup \Omega_2 \cup \Omega_3 \cup \Omega_4 \cup \Omega_5$ with

$$
\begin{aligned}
\Omega_1 &= \{D_1^-, D_1^- + h, D_1^- + 2h, \cdots, D_1^+\},\\
\Omega_2 &= \{D_2^-, D_2^- + (2h), \cdots, D_1^-\} \cup \{D_1^+, D_1^+ + (2h), \cdots, D_2^+\},\\
\Omega_3 &= \{D_3^-, D_3^- + (4h), \cdots, D_2^-\} \cup \{D_2^+, D_2^+ + (4h), \cdots, D_3^+\},\\
\Omega_4 &= \{D_4^-, D_4^- + (8h), \cdots, D_3^-\} \cup \{D_3^+, D_3^+ + (8h), \cdots, D_4^+\},\\
\Omega_5 &= \{0, 0.5D_4^-, D_4^-\} \cup \{D_4^+, D_4^+ + 0.5(L - D_4^+), L\}.
\end{aligned}
\tag{20}
$$

Here, $D_i^{\pm}$ are the upper and lower bounds of each uniform mesh and are defined as follows:

$$
\begin{aligned}
D_1^- &= K_1 - (0.5 + m_1)h, D_1^+ = K_1 + (0.5 + m_1)h,\\
D_2^- &= D_1^- - (2h)m_2, D_2^+ = D_1^+ + (2h)m_2,\\
D_3^- &= D_2^- - (4h)m_3, D_3^+ = D_2^+ + (4h)m_3,\\
D_4^- &= D_3^- - (8h)m_4, D_4^+ = D_3^+ + (8h)m_4,
\end{aligned}
\tag{21}
$$

where $2 \times m_i$ is the number of points in mesh Ω_i for $i = 1, 2, 3, 4$. In particular, $m_4 = \lfloor D_3^-/(8h) \rfloor - 1$ where $\lfloor x \rfloor$ is the maximum integer not greater than x. From now on, we use $m_1 = 5$, $m_2 = 5$, and $m_3 = 4$ in our numerical experiments. Figure 7 shows the piecewise-uniform mesh structure defined as Ω_x for pricing the three-asset cash-or-nothing option considered in this section. $d_i^{\pm}$, which is defined in Figure 7, is an index of the point x with the $D_i^{\pm}$ values defined above.

```
1 c l e a r ; c l c ;
2 L=200; x v o l=0. 3 ; y v o l=0. 3 ; z v o l=0. 3 ; r=0. 0 3 ; rho xy=0. 5 ; rho yz=0. 5 ;
3 rho zx=0. 5 ;K1=100;K2=100;K3=100;T=0.1 ; dt=0.1 /80;Nt=c e i l (T/dt ) ;
4 h=1;m1=5;m2=5;m3=4; xr=K1+0. 5 *h : h :K1+0. 5 *h+m1;
5 xr=[ xr (1:end -1) xr(end): 2 * h : xr(end)+2*h*m2 ] ;
6 xr=[ xr (1:end -1) xr(end): 4 * h : xr(end)+4*h*m3 ] ;
7 m4=f l o o r ( (L- xr(end)) /8) ;
8 xr=[ xr (1:end -1) xr(end): 8 * h : xr(end)+8*h*m4 ] ;
9 i f xr(end)<L
10 xr(end)=(xr ( end -1 )+L) / 2 ; xr ( end+1)=L;
11 end
12 x=[ f l i p l r (L- xr ) xr ] ; y=x ; z=x ;
13 Nx=length ( x ) ;Ny=length ( y ) ;Nz=length ( z ) ; hx=d i f f ( x ) ; hy=d i f f ( y ) ;
14 hz=d i f f ( z ) ;
15 U=z e r o s (Nx,Ny,Nz ,Nt+1) ;U( x>=K1, y>=K2, z>=K3, 1 ) =100;V=U;
16 alp=0. 5 ; s=1. 0 /( dt^ alp *gamma(2 - alp ) ) ;
17 ax=z e r o s (1 ,Nx-2 ) ; dx=ax ; cx=ax ;
18 f o r i =2:Nx-1
19 ax ( i -1 )=r *x ( i ) *hx( i ) /(hx( i -1 ) *(hx ( i -1 )+hx ( i ) ) ) . . .
20 - ( x v o l *x ( i ) ) ^2/(hx ( i -1 ) *( hx( i -1 )+hx ( i ) ) ) ;
21 dx ( i -1 )=s+( x v o l *x ( i ) ) ^2/(hx( i -1 ) *hx ( i ) ) . . .
22 - r *x ( i ) *( hx( i ) -hx( i -1 ) ) /(hx ( i -1 ) *hx( i ) )+r / 3 ;
23 cx ( i -1 )=- r *x ( i ) *hx ( i -1 ) /(hx ( i ) *(hx ( i -1 )+hx( i ) ) ) . . .
24 - ( x v o l *x ( i ) ) ^2/(hx ( i ) *(hx ( i -1 )+hx ( i ) ) ) ;
25 end
26 dx ( 1 )=dx ( 1 )++2*ax ( 1 ) ; cx ( 1 )=cx ( 1 ) - ax ( 1 ) ;
27 ax (Nx-2 )=ax (Nx-2 ) - cx (Nx-2 ) ; dx (Nx-2 )=dx(Nx-2 )++2*cx (Nx-2 ) ;
28 bx=ax ; by=ax ; bz=ax ;
29 f o r n=1:Nt
30 F=z e r o s (Nx-2 ,Ny-2 ,Nz -2 ) ;
31 i f n>1
32 f o r j =1:n -1
33 F=F+((n - j+1) ^(1 - alp ) - (n - j ) ^(1 - alp ) ) *(U( 2 :Nx-1 , 2 :Ny-1 , 2 :Nz -1 , j+1) . . .
34 -U( 2 :Nx-1 , 2 :Ny-1 , 2 :Nz -1 , j ) ) ;
35 end
36 end
37 V( : , : , : , n)=U( : , : , : , n) ;
38 f o r j =2:Ny-1
39 f o r k=2:Nz -1
40 f o r i =2:Nx-1
41 bx ( i -1 )=s *V( i , j , k , n) - s *F( i -1 , j -1 , k -1 ) . . .
42 +( rho xy * x v o l * y v o l *x ( i ) *y ( j ) *(V( i +1, j +1,k , n)+V( i -1 , j -1 , k , n) . . .
43 -V( i -1 , j+1,k , n) -V( i +1, j -1 , k , n) ) / ( ( hx ( i ) *hy( j ) )+(hx ( i -1 ) *hy ( j ) ) . . .
44 +(hx( i ) *hy( j -1 ) )+(hx ( i -1 ) *hy( j -1 ) ) ) . . .
45 +rho yz * y v o l * z v o l *y ( j ) *z ( k ) *(V( i , j+1,k+1,n)+V( i , j -1 , k -1 , n) . . .
46 -V( i , j -1 , k+1,n) -V( i , j +1,k -1 , n) ) / ( ( hy ( j ) *hz ( k ) )+(hy ( j -1 ) *hz ( k ) ) . . .
47 +(hy( j ) *hz ( k -1 ) )+(hy ( j -1 ) *hz ( k -1 ) ) ) . . .
48 +rho zx * x v o l * z v o l *x ( i ) *z ( k ) *(V( i +1, j , k+1,n)+V( i -1 , j , k -1 , n) . . .
49 -V( i -1 , j , k+1,n) -V( i +1, j , k -1 , n) ) / ( ( hx ( i ) *hz ( k ) )+(hx ( i -1 ) *hz ( k ) ) . . .
50 +(hx( i ) *hz ( k -1 ) )+(hx ( i -1 ) *hz ( k -1 ) ) ) ) ;
51 end
52 U( 2 :Nx-1 , j , k , n+1)=thomas3 ( ax , dx , cx , bx ) ;
53 end
54 end
55 U( 1 , 2 :Ny-1 , 2 :Nz -1 , n+1)=2*U( 2 , 2 :Ny-1 , 2 :Nz -1 , n+1) . . .
56 -U( 3 , 2 :Ny-1 , 2 :Nz -1 , n+1) ;
57 U( : , 1 , 2 :Nz -1 , n+1)=2*U( : , 2 , 2 :Nz -1 , n+1) -U( : , 3 , 2 :Nz -1 , n+1) ;
58 U( : , : , 1 , n+1)=2*U( : , : , 2 , n+1) -U( : , : , 3 , n+1) ;
59 U(Nx , 2 :Ny-1 , 2 :Nz -1 , n+1)=2*U(Nx-1 , 2 :Ny-1 , 2 :Nz -1 , n+1) . . .
60 -U(Nx-2 , 2 :Ny-1 , 2 :Nz -1 , n+1) ;
```

Listing 1: Continued.

```
61 U( : ,Ny , 2 :Nz -1 , n+1)=2*U( : ,Ny-1 , 2 :Nz -1 , n+1) -U( : ,Ny-2 , 2 :Nz -1 , n+1) ;
62 U( : , : ,Nz , n+1)=2*U( : , : ,Nz -1 , n+1) -U( : , : ,Nz -2 , n+1) ;
63 f o r k=2:Nz -1
64 f o r i =2:Nx-1
65 f o r j =2:Ny-1
66 by ( j -1 )=s *U( i , j , k , n+1) ;
67 end
68 V( i , 2 :Ny-1 , k , n+1)=thomas3 ( ax , dx , cx , by ) ;
69 end
70 end
71 V( 1 , 2 :Ny-1 , 2 :Nz -1 , n+1)=2*V( 2 , 2 :Ny-1 , 2 :Nz -1 , n+1) . . .
72 -V( 3 , 2 :Ny-1 , 2 :Nz -1 , n+1) ;
73 V( : , 1 , 2 :Nz -1 , n+1)=2*V( : , 2 , 2 :Nz -1 , n+1) -V( : , 3 , 2 :Nz -1 , n+1) ;
74 V( : , : , 1 , n+1)=2*V( : , : , 2 , n+1) -V( : , : , 3 , n+1) ;
75 V(Nx , 2 :Ny-1 , 2 :Nz -1 , n+1)=2*V(Nx-1 , 2 :Ny-1 , 2 :Nz -1 , n+1) . . .
76 -V(Nx-2 , 2 :Ny-1 , 2 :Nz -1 , n+1) ;
77 V( : ,Ny , 2 :Nz -1 , n+1)=2*V( : ,Ny-1 , 2 :Nz -1 , n+1) -V( : ,Ny-2 , 2 :Nz -1 , n+1) ;
78 V( : , : ,Nz , n+1)=2*V( : , : ,Nz -1 , n+1) -V( : , : ,Nz -2 , n+1) ;
79 f o r j =2:Ny-1
80 f o r i =2:Nx-1
81 f o r k=2:Nz -1
82 bz (k -1 )=s *V( i , j , k , n+1) ;
83 end
84 U( i , j , 2 :Nz -1 , n+1)=thomas3 ( ax , dx , cx , bz ) ;
85 end
86 end
87 U( 1 , 2 :Ny-1 , 2 :Nz -1 , n+1)=2*U( 2 , 2 :Ny-1 , 2 :Nz -1 , n+1) . . .
88 -U( 3 , 2 :Ny-1 , 2 :Nz -1 , n+1) ;
89 U( : , 1 , 2 :Nz -1 , n+1)=2*U( : , 2 , 2 :Nz -1 , n+1) -U( : , 3 , 2 :Nz -1 , n+1) ;
90 U( : , : , 1 , n+1)=2*U( : , : , 2 , n+1) -U( : , : , 3 , n+1) ;
91 U(Nx , 2 :Ny-1 , 2 :Nz -1 , n+1)=2*U(Nx-1 , 2 :Ny-1 , 2 :Nz -1 , n+1) . . .
92 -U(Nx-2 , 2 :Ny-1 , 2 :Nz -1 , n+1) ;
93 U( : ,Ny , 2 :Nz -1 , n+1)=2*U( : ,Ny-1 , 2 :Nz -1 , n+1) -U( : ,Ny-2 , 2 :Nz -1 , n+1) ;
94 U( : , : ,Nz , n+1)=2*U( : , : ,Nz -1 , n+1) -U( : , : ,Nz -2 , n+1) ;
95 end
96 f i g u r e ( 1 ) ; c l f ; colormap ( [ 0 0 0 ] ) ;
97 mesh ( x , y ,U( : , : , min ( f i n d ( z>100) )++1,n+1) ) ;
98 Pr i c e=i n t e rp 3 (y , x , z ,U( : , : , : , Nt+1) ,K1,K2,K3)
99 f u n c t i on x=thomas3 ( alpha , beta ,gamma, f )
100 n=length ( f ) ;
101 f o r i =2:n
102 mult=alpha ( i ) / be ta ( i -1 ) ;
103 be ta ( i )=be ta ( i ) -mult*gamma( i -1 ) ;
104 f ( i )=f ( i ) -mult* f ( i -1 ) ;
105 end
106 x (n)=f (n) / be ta (n) ;
107 f o r i=n -1 : -1 : 1
108 x ( i )=( f ( i ) -gamma( i ) *x ( i+1) ) / be ta ( i ) ;
109 end
110 end
```

Listing 1: MATLAB code for cash-or-nothing.

Given the same option, Table 2 lists the option prices with respect to α. Here, $h = 1$ and $\Delta\tau = 0.1/80$ are taken and the other parameters are the same as in the test above. The code for the numerical implementation for this test is provided in the appendix.

Figure 8 shows the option prices according to the value of α. For $T = 0.1$, the option prices obtained tend to be undervalued as α decreases, as is the case with one underlying asset.

Figure 9 shows the CPU time and prices of three-asset cash-or-nothing option. In Figure 9, the dotted curve is the reference price of using the uniform mesh with mesh size $h = 1$. We use the maturity time $T = 0.1$, and the other parameters are the same as in the tests previously. In Figure 9, the solid and dashed curves are the CPU time and prices, respectively, with respect to uniform mesh with mesh size $h = 2, 3, \cdots, 8$. Here, the uniform mesh is

constructed as shown in Figure 6. Figure 10 was constructed in a similar manner to Figure 7. Here, we add a piecewise-uniform mesh with a step size $16h$. Likewise, we define $D_5^{\pm} = D_4^{\pm} \pm (16h)m_5$, and $m_5 = \lfloor D_4^{-}/(16h) \rfloor - 1$. We compute the CPU time and price of using the nonuniform mesh with $m_1 = 1, m_2 = 2, m_3 = 3$, and $m_4 = 1$, which is constructed in Figure 10. We can confirm that the difference between the reference and numerical solutions obtained with each mesh is greater when using the uniform mesh, despite using the number of same grid points when the uniform mesh size is $h = 8$. Additionally, the elapsed time is similar to using the uniform mesh. In other words, nonuniform meshes are faster and more accurate compared to uniform mesh.

3.2.2. Equity-Linked Security. We consider a three-asset equity-linked security (ELS) option that contains knock-in-barrier (D). The complex profit structure of ELS complicates pricing. To briefly explain return of ELS on one asset, if the underlying asset price is higher than the predetermined exercise prices $(K_1, K_2, \cdots, K_6)$ on the early exercise date before maturity, the contract provides the specific returns $(c_1, c_2, \cdots, c_6)$ and is terminated. Otherwise, the contract will continue on the next early exercise date. If the contract is not terminated by maturity, it depends on whether the underlying asset touched the knock-in-barrier. If the underlying asset did not touch the knock-in-barrier, it provides dummy return (d) and otherwise suffers losses. The payoff structure of ELS is illustrated in Figure 11.

For $\alpha = 0.8$, we performed the comparison test with the uniform mesh under the same conditions considered in Section 3.2 [35] on the nonuniform mesh. For additional information on numerical testing, please refer to the thesis [35]. The nonuniform mesh was constructed using the piecewise-uniform mesh, as shown in Figure 12, with fixed points $(0, D/2, D, K_1, K_2, \cdots, K_6, x0, L)$ and $m_1 = 5, m_2 = 20$, where $x0$ is the current underlying price.

When using a nonuniform grid as shown in Figure 12, the ELS price is 8767 and the elapsed time is 15.3783. When comparing this result to the result obtained using the uniform mesh ($h = 2$), the relative error of the price is 0.0205 and the elapsed time is 470 times shorter.

4. Conclusions

In this study, we presented an efficient and accurate nonuniform FDM for the 3D time-fractional BS equation. In numerical experiments, we investigated the effects of the fractional-order α by considering one-asset cash-or-nothing European call option. The lower the value of α, and the shorter the maturity of the option, and the larger the difference in option prices between the $\alpha = 1.0$ and $\alpha < 1.0$ except for at the money (ATM). Because of the complexity of calculations and CPU time for computation on high-dimensional options takes longer, there is a lack of research on higher-dimensional numerical methods with more than three assets in the time-fractional BS equation. We used the nonuniform implicit FDM with operator splitting scheme for pricing three-asset cash-or-nothing options and ELS. Here, we use the operator splitting method to solve the discrete system of equations and linear boundary conditions efficiently. Based on the use of the nonuniform implicit FDM, the numerical solution computation could be fast, and the numerical scheme could be stable even if relatively large time steps are used. Our results suggest that the proposed method is faster and more accurate than the uniform mesh. We demonstrated the efficiency and fastness of the proposed method through numerical experiments. Although there have been theoretical analyses (stability analysis, truncation error, and convergence analysis) of the one-dimensional time-fractional BS equation [1, 27], there is a lack of research on multidimensional theoretical analysis of the time-fractional BS equation. Therefore, for future work, we will perform the theoretical analysis of the multidimensional time-fractional BS equation and compute various financial assets based on the multidimensional time-fractional BS equation using the proposed method and continue to improve our method.

Appendix

The following Listing 1 is a MATLAB code for pricing the three-asset cash-or-nothing European call option.

Data Availability

No data were used to support this study.

Conflicts of Interest

The authors declare that they have no conflicts of interest.

Acknowledgments

The corresponding author (J.S. Kim) was supported by the Brain Korea 21 FOUR from the Ministry of Education of the Republic of Korea.

References

[1] J. Huang, Z. Cen, and J. Zhao, "An adaptive moving mesh method for a time-fractional Black–Scholes equation," *Advances in Difference Equations*, vol. 2019, no. 1, 14 pages, 2019.

[2] F. Black and M. Scholes, "The pricing of options and corporate liabilities," *Journal of Political Economy*, vol. 81, no. 3, pp. 637–654, 1973.

[3] A. A. Tateishi, H. V. Ribeiro, and E. K. Lenzi, "The role of fractional time-derivative operators on anomalous diffusion," *Frontiers in Physics*, vol. 5, 2017.

[4] Y. Chen, H. Gu, and L. Ma, "Variational method to -Laplacian fractional Dirichlet problem with instantaneous and noninstantaneous impulses," *Journal of Function Spaces*, vol. 2020, Article ID 8598323, 8 pages, 2020.

[5] D. Prathumwan and K. Trachoo, "On the solution of two-dimensional fractional Black–Scholes equation for European put option," *Advances in Difference Equations*, vol. 2020, no. 1, 9 pages, 2020.

[6] Y. Kumar and V. K. Singh, "Computational approach based on wavelets for financial mathematical model governed by distributed order fractional differential equation," *Mathematics and Computers in Simulation*, vol. 190, pp. 531–569, 2021.

[7] M. X. Zhou, A. S. V. Kanth, K. Aruna et al., "Numerical solutions of time fractional Zakharov-Kuznetsov equation via natural transform decomposition method with nonsingular kernel derivatives," *Journal of Function Spaces*, vol. 2021, Article ID 9884027, 17 pages, 2021.

[8] S. Kumar, A. Yildirim, Y. Khan, H. Jafari, K. Sayevand, and L. Wei, "Analytical solution of fractional Black–Scholes European option pricing equation by using Laplace transform," *Journal of Fractional Calculus and Applications*, vol. 2, no. 8, pp. 1–9, 2012.

[9] J. S. Duan, L. Lu, L. Chen, and Y. L. An, "Fractional model and solution for the Black–Scholes equation," *Mathematical Methods in the Applied Sciences*, vol. 41, no. 2, pp. 697–704, 2018.

[10] K. Zhang, "Existence and uniqueness of analytical solution of time-fractional Black–Scholes type equation involving hyper-Bessel operator," *Mathematical Methods in the Applied Sciences*, vol. 44, no. 7, pp. 6164–6177, 2021.

[11] M. M. Khader, "The numerical solution for BVP of the liquid film flow over an unsteady stretching sheet with thermal radiation and magnetic field using the finite element method," *International Journal of Modern Physics C*, vol. 30, no. 11, pp. 1950080–1950088, 2019.

[12] Y. Gu and H. Sun, "A meshless method for solving three-dimensional time fractional diffusion equation with variable-order derivatives," *Applied Mathematical Modelling*, vol. 78, pp. 539–549, 2020.

[13] P. Roul, "A high accuracy numerical method and its convergence for time-fractional Black-Scholes equation governing European options," *Applied Numerical Mathematics*, vol. 151, pp. 472–493, 2020.

[14] M. M. Khader, "Fourth-order predictor-corrector FDM for the effect of viscous dissipation and Joule heating on the Newtonian fluid flow," *Computers & Fluids*, vol. 182, pp. 9–14, 2019.

[15] M. M. Khader and R. P. Sharma, "Evaluating the unsteady MHD micropolar fluid flow past stretching/shirking sheet with heat source and thermal radiation: implementing fourth order predictor-corrector FDM," *Mathematics and Computers in Simulation*, vol. 181, pp. 333–350, 2021.

[16] H. Zhang, F. Liu, S. Chen, and M. Shen, "A fast and high accuracy numerical simulation for a fractional Black–Scholes model on two assets," *Annals of Applied Mathematics*, vol. 36, no. 1, pp. 91–110, 2020.

[17] W. Wyss, "The fractional Black–Scholes equation," *Fractional Calculus and Applied Analysis*, vol. 3, no. 1, pp. 51–61, 2000.

[18] W. Chen, X. Xu, and S. P. Zhu, "Analytically pricing double barrier options based on a time-fractional Black- Scholes equation," *Computers & Mathematics with Applications*, vol. 69, no. 12, pp. 1407–1419, 2015.

[19] A. N. Fall, S. N. Ndiaye, and N. Sene, "Black-Scholes option pricing equations described by the Caputo generalized fractional derivative," *Chaos, Solitons & Fractals*, vol. 125, pp. 108–118, 2019.

[20] A. A. Khajehnasiri and M. Safavi, "Solving fractional Black-Scholes equation by using Boubaker functions," *Mathematical Methods in the Applied Sciences*, vol. 4, no. 11, pp. 8505–8515, 2021.

[21] C. Chen, Z. Wang, and Y. Yang, "A new operator splitting method for American options under fractional Black- Scholes models," *Computers & Mathematics with Applications*, vol. 77, no. 8, pp. 2130–2144, 2019.

[22] G. Krzyżanowski, M. Magdziarz, and Ł. Płociniczak, "A weighted finite difference method for subdiffusive Black-Scholes model," *Computers & Mathematics with Applications*, vol. 80, no. 5, pp. 653–670, 2020.

[23] X. Chen, D. Ding, S. L. Lei, and W. Wang, "A fast preconditioned iterative method for two-dimensional options pricing under fractional differential models," *Computers & Mathematics with Applications*, vol. 79, no. 2, pp. 440–456, 2020.

[24] S. E. Fadugba, "Homotopy analysis method and its applications in the valuation of European call options with time-fractional Black-Scholes equation," *Chaos, Solitons & Fractals*, vol. 141, article 110351, 2020.

[25] L. Song, "A space-time fractional derivative model for European option pricing with transaction costs in fractal market," *Chaos, Solitons & Fractals*, vol. 103, pp. 123–130, 2017.

[26] X. Zhang, S. Shuzhen, W. Lifei, and Y. Xiaozhong, "θ-Difference numerical method for solving time-fractional Black–Scholes equation. Highlights of Science paper online," *China Science and Technology Papers*, vol. 7, no. 13, pp. 1287–1295, 2014.

[27] R. H. De Staelen and A. S. Hendy, "Numerically pricing double barrier options in a time-fractional Black-Scholes model," *Computers & Mathematics with Applications*, vol. 74, no. 6, pp. 1166–1175, 2017.

[28] A. Golbabai and O. Nikan, "A computational method based on the moving least-squares approach for pricing double barrier options in a time-fractional Black-Scholes model," *Computational Economics*, vol. 55, no. 1, pp. 119–141, 2020.

[29] M. S. Hashemi, M. Inc, and A. Yusuf, "On three-dimensional variable order time fractional chaotic system with nonsingular kernel," *Chaos, Solitons & Fractals*, vol. 133, article 109628, 2020.

[30] M. She, L. Li, R. Tang, and D. Li, "A novel numerical scheme for a time fractional Black-Scholes equation," *Journal of Applied Mathematics and Computing*, vol. 66, no. 1-2, pp. 853–870, 2021.

[31] Z. Tian, S. Zhai, H. Ji, and Z. Weng, "A compact quadratic spline collocation method for the time-fractional Black-Scholes model," *Journal of Applied Mathematics and Computing*, vol. 66, no. 1-2, pp. 327–350, 2021.

[32] W. Chen and S. Wang, "A 2nd-order ADI finite difference method for a 2D fractional Black-Scholes equation governing European two asset option pricing," *Mathematics and Computers in Simulation*, vol. 171, pp. 279–293, 2020.

[33] J. Bodeau, G. Riboulet, and T. Roncalli, "Non-uniform grids for PDE in finance," 2000, https://papers.ssrn.com/sol3/papers.cfm?abstract_id=1031941.

[34] S. Kim, D. Jeong, C. Lee, and J. Kim, "Finite difference method for the multi-asset Black–Scholes equations," *Mathematics*, vol. 8, no. 3, p. 391, 2020.

[35] W. Lee, *An efficient finite difference method for the three-dimensional time-fractional Black–Scholes equation*, Graduate School, Korea University, 2021.